

Enhanced Two-Photon Processes in Quantum Dots inside Photonic Crystal Nanocavities and Quantum Information Science Applications

Ziliang Lin* and Jelena Vučković

E. L. Ginzton Laboratory, Stanford University, Stanford, CA 94305, USA

(Dated: November 25, 2021)

We show that the two-photon transition rates of quantum dots coupled to nanocavities are enhanced by up to 8 orders of magnitude relative to quantum dots in bulk host. We then propose how to take advantage of this enhancement to implement coherent quantum dot excitation by two-photon absorption, entangled photon pair generation by two-photon spontaneous emission, and single-photon generation at telecom wavelengths by two-photon stimulated and spontaneous emission.

Recent progress in semiconductor quantum dots (QDs) coupled to photonic crystal (PC) cavities has shown that these systems exhibit cavity quantum electrodynamics effects. Experiments have demonstrated creation of single photons in the near infrared[1], Purcell enhancement of QD spontaneous emission rates in weak coupling regime[2, 3], polariton state splitting in strong coupling regime[4, 5, 6], controlled amplitude and phase shifts at a single photon level[7], and photon induced tunneling and blockade[8]. These results indicate that the QDs can be combined with PC cavities in an integrated platform for quantum information science[9, 10, 11].

However, many important challenges remain in the QD-PC cavity systems. Among them is the generation of indistinguishable single photons, preferably at telecom wavelengths. This challenge results from the fact that an incoherently excited QD has to undergo phonon assisted relaxation to its lowest excited state, so the single photons it emits have different temporal profiles[12, 13]. For this reason, the maximum demonstrated indistinguishability between photons emitted from a single QD has been around 81%[14]. This problem would be resolved by exciting QDs coherently. In addition, coherent excitation is of great interest for quantum information science, as it also enables manipulation of QD states. However, this type of excitation experiments face the difficulty of separating signal and probe photons that have the same wavelength. Another challenge is the generation of entangled photon pairs[15]. Although photon pairs can be created from biexciton decay cascade in a QD[16, 17], the pairs are not entangled in polarization because the intermediate exciton states are split by anisotropic electron-hole exchange interactions[18, 19].

In this Letter, we analyze two-photon absorption (TPA) and emission (TPE) in QDs coupled to PC cavities as solutions to these challenges (Fig. 1). TPA allows coherent excitation of the QDs when the frequencies of the two photons are tuned such that their sum matches the transition frequency of the QDs, and at the same time allows for the frequency separation of the signal and probe photons. Hence, TPA can eliminate jitter in single photon generation from a QD. On the other hand, TPE from an excited QD allows the generation of single photons and entangled photon pairs on demand at telecom wavelengths. We also show that semiconductor QDs coupled to PC cavities enable great enhancement of two-photon tran-

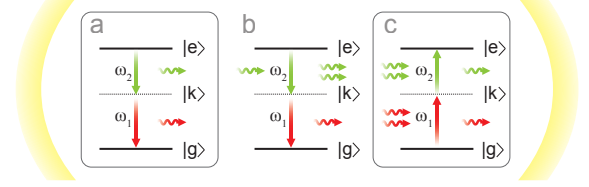


FIG. 1: (Color online) (a) Spontaneous emission of a pair of photons from an excited QD via a virtual state. (b) Stimulated two-photon emission from an excited QD. The first photon emission is stimulated with an external laser and the second photon emission is spontaneous. (c) Two-photon absorption by a QD. In all three processes, the transition rates are enhanced inside a single-mode or double-mode cavity (pictured here as a generic cavity) matching the photon frequencies.

sition rates relative to slow rates in bulk host[20, 21, 22].

We model the semiconductor QD as a two-level system with energy separation $\hbar\omega_d$, where \hbar is the reduced Planck's constant. The QD is illuminated by two laser beams of frequencies ω_1 and ω_2 . By applying time-dependent perturbation theory, we obtain the nondegenerate two-photon transition rate from the ground state to the excited state: $\gamma = 2\pi|\Omega_{\text{eff}}|^2\delta(\omega_d - \omega_1 - \omega_2)$, where the effective Rabi rate is

$$\Omega_{\text{eff}} = \sum_k \left[\frac{\Omega_{gk,1}\Omega_{ke,2}}{\Delta_{gk,1}} + \frac{\Omega_{gk,2}\Omega_{ke,1}}{\Delta_{gk,2}} \right]. \quad (1)$$

The summation is performed over all the virtual intermediate states $|k\rangle$'s. $\Omega_{gk,1}$ ($\Omega_{gk,2}$) is the Rabi transition rate between the ground state and the intermediate state driven by the laser with frequency ω_1 (ω_2). $\Delta_{gk,1}$ is the QD-light detuning $\omega_k - \omega_g - \omega_1$, and a similar expression holds for $\Delta_{gk,2}$. The delta function represents energy conservation. It must be pointed out that although Eqn. (1) describes TPA rates, TPE rate expression holds the same form with $\Delta_{gk,1}$ ($\Delta_{gk,2}$) replaced by $\Delta_{ke,2}$ ($\Delta_{ke,1}$). We start from the expression for two-photon Rabi frequency for an excited QD with quantized electric field:

$$\Omega_{gk,1} = \frac{|\mathbf{d}_{gk}|}{\hbar} \left[\frac{(N_1 + 1)\hbar\omega_1}{2n^2\epsilon_0 V_1} \right]^{1/2} \psi_{gk,1}, \quad (2)$$

where \mathbf{d}_{gk} is the transition dipole moment. N_1 and V_1 are photon number and volume of the mode at frequency ω_1 that the

QD is interacting with. n is refractive index of the host substrate and ε_0 is the free space permittivity. $\psi_{gk,1}$ characterizes the reduction in Rabi rate due to position mismatch between the QD and the electric field maximum within the cavity: $\psi_{gk,1} = \frac{|\mathbf{E}_1(\mathbf{r})|}{|\mathbf{E}_1(\mathbf{r}_M)|} \left(\frac{\mathbf{d}_{gk} \cdot \mathbf{e}_1}{|\mathbf{d}_{gk}|} \right)$, where $\mathbf{E}_1(\mathbf{r})$ is the electric field at the QD location, $|\mathbf{E}_1(\mathbf{r}_M)|$ is the maximum field strength in the cavity, and \mathbf{e}_1 is the polarization of the field. Similar expressions hold for Rabi rates $\Omega_{ke,1}$, $\Omega_{gk,2}$, and $\Omega_{ke,2}$.

By combining Eqs. (1) and (2), we can write the expression for nondegenerate two photon transition rate as:

$$\gamma = 2\pi \frac{\omega_1 \omega_2 (N_1 + 1)(N_2 + 1)}{(2\hbar n^2 \varepsilon_0)^2 V_1 V_2} M_{12}^2 \delta(\omega_d - \omega_1 - \omega_2), \quad (3)$$

with

$$M_{12} = \left| \sum_k \left[\frac{|\mathbf{d}_{gk}| |\mathbf{d}_{ke}| \psi_{gk,1} \psi_{ke,2}}{\Delta_{gk,1}} + \frac{|\mathbf{d}_{gk}| |\mathbf{d}_{ke}| \psi_{gk,2} \psi_{ke,1}}{\Delta_{gk,2}} \right] \right|.$$

In Eqs. (2) and (3), for spontaneous emission we set $N_1 = 0$, for stimulated emission we keep $N_1 + 1$ term, and for absorption we replace $N_1 + 1$ with N_1 . To obtain the total two-photon spontaneous emission (TPSE) rate Γ^{TPSE} (Fig. 1a), we need to integrate Eqn. (3) over all frequencies: $\partial \Gamma^{\text{TPSE}} / \partial \omega_2 = \int d\omega_1 \gamma \rho(\omega_1) \rho(\omega_2)$, where ρ 's are the photon densities of states. By setting $N_1 = N_2 = 0$, we obtain

$$\frac{\partial \Gamma^{\text{TPSE}}}{\partial \omega_2} = \frac{2\pi}{(2\hbar n^2 \varepsilon_0)^2 V_1 V_2} \omega_1 \omega_2 \rho(\omega_1) \rho(\omega_2) M_{12}^2.$$

We arrive at our final expression by writing explicitly the density of states $\rho(\omega)$. In bulk, $\rho(\omega_1) = V_1 n^3 \omega_1^2 / (3\pi^2 c^3)$. For a cavity $\omega_1 \rho(\omega_1) = 2Q_1 \phi_1 / \pi$, where Q_1 is the cavity quality factor and ϕ_1 characterizes frequency mismatch between ω_1 and cavity resonance frequencies ω_{1c} , $\phi_1(\omega_1) = \frac{\omega_1 / \omega_{1c}}{1 + 4Q_1^2 (\omega_1 / \omega_{1c} - 1)^2}$. Finally, the TPSE rates for a QD in bulk semiconductor host ($\Gamma_0^{\text{TPSE}}(\omega_1, \omega_2)$) and in a double-mode cavity centered at ω_{1c} and ω_{2c} ($\Gamma_{\omega_{1c}, \omega_{2c}}^{\text{TPSE}}(\omega_1, \omega_2)$) are

$$\begin{aligned} \frac{\partial \Gamma_0^{\text{TPSE}}}{\partial \omega_2} &= \frac{\pi}{2} \left[\frac{n\omega_1^3}{3\pi^2 \hbar \varepsilon_0 c^3} \right] \left[\frac{n\omega_2^3}{3\pi^2 \hbar \varepsilon_0 c^3} \right] M_{12}^2 \text{ with all } \psi\text{'s} = 1, \\ \frac{\partial \Gamma_{\omega_{1c}, \omega_{2c}}^{\text{TPSE}}}{\partial \omega_2} &= \frac{\pi}{2} \left[\frac{2Q_1 \phi_1}{\pi \hbar n^2 \varepsilon_0 V_1} \right] \left[\frac{2Q_2 \phi_2}{\pi \hbar n^2 \varepsilon_0 V_2} \right] M_{12}^2 \end{aligned} \quad (4)$$

with the energy conservation condition $\omega_1 + \omega_2 = \omega_d$.

Physically, TPSE occurs as the result of the interaction between the excited QD and the vacuum states of the electromagnetic field with modes frequencies ω_1 and ω_2 . Since there is a series of (ω_1, ω_2) satisfying the energy conservation condition, the TPSE spectrum of a single QD is broad. Furthermore, the TPSE rate is slower than the one-photon emission because virtual states are required for it. The combination of broad spectrum and low transition rate results in an overall low signal intensity, and therefore TPSE is generally difficult to detect.

However, the TPSE rate is enhanced when the QD is placed inside a cavity, because the cavity modifies the photon density of states in free space into a Lorentzian distribution and also localizes field into small volume which leads to stronger interaction. This rate enhancement is similar to the one-photon spontaneous emission rate enhancement discovered by Purcell[23]. The two-photon rate enhancement in a double-mode cavity relative to the bulk medium can be seen by taking the ratio of Eqs. (4):

$$\frac{\Gamma_{\omega_{1c}, \omega_{2c}}^{\text{TPSE}}}{\Gamma_0^{\text{TPSE}}} = F_1 F_2 = \left[\frac{3}{4\pi^2} \left(\frac{\lambda_1}{n} \right)^3 \frac{Q_1 \phi_1}{V_1} \right] \left[\frac{3}{4\pi^2} \left(\frac{\lambda_2}{n} \right)^3 \frac{Q_2 \phi_2}{V_2} \right],$$

where F_1 (F_2) and λ_1 (λ_2) are the Purcell factor and free-space wavelength for frequency ω_1 (ω_2), respectively. It should be noted that this expression corresponds to the maximum enhancement, assuming the QD is located at the field maxima for both modes (i.e. all ψ 's = 1).

Experimentally, single-mode cavities with Q 's exceeding 10^4 and mode volumes below cubic optical wavelength have been demonstrated, and doubly resonant cavities with similar Q 's and mode volumes are possible[24]. Therefore, we expect the QD TPSE to be increased by up to 4 orders of magnitude in single-mode cavities and by 8 orders of magnitude in double-mode cavities. Second, in photonic crystal cavities only the emission rates with frequency pair (ω_1, ω_2) matching the cavity frequencies $(\omega_{1c}, \omega_{2c})$ are enhanced while emission rates with other frequency pairs are greatly suppressed as a result of the reduction in photon density of states relative to the bulk medium. Thus, the cavities offer good controls over the frequencies of emitted photons. Third, inside a double-mode cavity with degenerate polarizations for both modes, the two emitted photons are entangled in polarization.

Similarly, we can address the problem of cavity enhanced TPA (Fig. 1c). For bulk, combining $n^2 \varepsilon_0 |\mathbf{E}_1|^2 V_1 = N_1 \hbar \omega_1$ and $2n \varepsilon_0 c |\mathbf{E}_1|^2 A_1 = P_1$, we obtain $N_1 \hbar \omega_1 = P_1 V_1 n / (2c A_1)$, where A_1 is the laser beam spot radius. For laser coupled to cavity mode, $N_1 \hbar \omega_1 = \eta_1 P_1 Q_1 \phi_1 / \omega_1$. Similar expressions hold for ω_2 . By substituting expressions for $N_i \hbar \omega_i$ into Eqn. (3), the TPA rates in bulk and double-mode cavity are, respectively:

$$\begin{aligned} \gamma_0^{\text{TPA}} &= \frac{\pi}{2} \left[\frac{P_1}{2\hbar^2 n \varepsilon_0 c A_1} \right] \left[\frac{P_2}{2\hbar^2 n \varepsilon_0 c A_2} \right] M_{12}^2 \delta(\omega_d - \omega_1 - \omega_2), \\ \gamma_{\omega_{1c}, \omega_{2c}}^{\text{TPA}} &= \frac{\pi}{2} \left[\frac{\eta_1 P_1 Q_1 \phi_1}{2\hbar^2 \omega_1 n^2 \varepsilon_0 V_1} \right] \left[\frac{\eta_2 P_2 Q_2 \phi_2}{2\hbar^2 \omega_2 n^2 \varepsilon_0 V_2} \right] M_{12}^2 \delta(\omega_d - \omega_1 - \omega_2). \end{aligned}$$

In the nondegenerate TPA, the absorption rate has a linear dependence on P_1 and P_2 . Similar to the TPSE rate, the TPA rate is enhanced because the cavity modifies the photon density of states. For the same excitation laser power and laser frequencies resonant with cavity mode frequencies, the rate enhancement is $\gamma_{\omega_{1c}, \omega_{2c}}^{\text{TPA}} / \gamma_0^{\text{TPA}} = G_1 G_2$, where $G_i = \eta_i Q_i A_i \lambda_i / (\pi V_i n)$.

Two-photon excitation of QDs holds several advantages over conventional one-photon excitation. By tuning ω_1 and

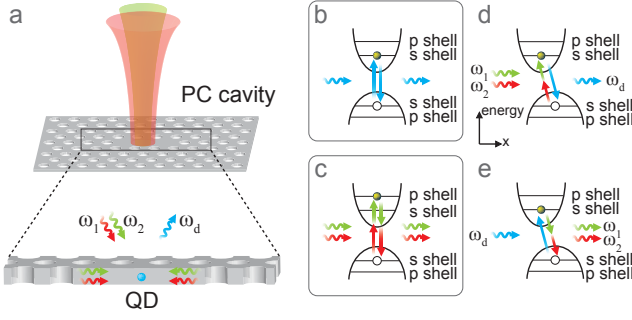


FIG. 2: (Color online) (a) Setup for enhanced two-photon absorption experiment: two laser beams with frequencies ω_1 and ω_2 are injected to a double-mode cavity. (b) and (c) Parity selection rules dictate that one-photon s shell- s shell transitions are allowed but two-photon s shell- s shell transitions are forbidden. However, two-photon s shell- p shell transitions are permitted. The p shell is approximately 10 meV above the s shell in InAs QDs[26]. (d) Enhanced two-photon absorption and single-photon generation in a QD with a DC lateral electric field applied to it along the x direction. The lateral electric field shifts apart the hole valence band and the electron conduction band and therefore breaks the parity selection rule. (e) Enhanced two-photon spontaneous emission in a QD as a reverse process of two-photon absorption. The one-photon excited electron recombines with the hole and generates entangled photon pairs at (1550, 2300) nm via two-photon spontaneous emission.

ω_2 to match $\omega_1 + \omega_2 = \omega_d$, we can coherently excite a QD and therefore create a source of indistinguishable single photons on demand. This is because we eliminate a 10-30 ps time jitter in emitted single photons[12]. Two-photon excitation also presents a solution to the separation of signal and probe photons, because the excitation and emission wavelengths are different. Finally, TPA offers a convenient tool to coherently excite and manipulate a QD, which is of interest for quantum information processing[25].

With similar calculations, we derive the two photon stimulated emission (TPSTE) rate in a double-mode cavity with stimulation by a laser beam with power P_2 and frequency ω_2 , whose coupling efficiency to the cavity mode is denoted as η_2 ,

$$\Gamma_{\omega_1, \omega_2}^{\text{TPSTE}} = \frac{\pi}{2} \left[\frac{2Q_1\phi_1}{\pi\hbar n^2 \varepsilon_0 V_1} \right] \left[\frac{\eta_2 P_2 Q_2 \phi_2}{2\hbar^2 \omega_2 n^2 \varepsilon_0 V_2} \right] M_{12}^2. \quad (5)$$

Fig. 1b shows the stimulated emission of a photon of frequency ω_2 and the spontaneous emission of a photon of frequency ω_1 . Eqn. (5) shows that the TPSTE rate is linearly dependent on the stimulation light power and the rate is increased by a factor of $\eta_2 P_2 \pi / (4\hbar\omega_2)$ compared to the TPSE rate. This additional enhancement makes the QD an selective single photon emitter at ω_1 .

We propose to experimentally demonstrate enhanced TPA and TPE in InAs QDs embedded in two-dimensional GaAs double-mode PC cavities (Fig. 2a). Since the QDs have ground and excited state splitting ranging from 900 nm to 950 nm, we select two photon wavelengths as $\lambda_1 = 1550$ nm and $\lambda_2 = 2300$ nm, conveniently coinciding with the telecom band (suitable for propagation down the fiber) and

emission from existing GaSb lasers, respectively. To generate indistinguishable single photons on demand, we excite a QD with TPA and collect single photons emitted at $\lambda_d = 926$ nm (Fig. 2d). To generate entangled photon pairs, we excite a QD with one-photon process and collect photon pairs at (1550, 2300) nm via TPSE (Fig. 2e). In addition, when we stimulate this excited QD with a 2300 nm laser beam, we can generate 1550 nm photons on demand via TPSTE.

An examination of M_{12} reveals that two-photon transitions have opposite parity selection rules relative to one-photon transitions. In one-photon transition, the ground and excited states need to have opposite parity so that $|\mathbf{d}_{ge}|$ is nonzero. On the other hand, a two-photon transition requires the ground and excited states having the same parity for $|\mathbf{d}_{gk}||\mathbf{d}_{ke}|$ to be nonzero. This selection rule discrepancy implies that two-photon transitions cannot connect states that have one-photon transitions and vice versa. For a QD in the effective mass approximation, its energy eigenfunctions can be written as a product of an periodic function $u(\mathbf{r})$ and an envelope function $f(\mathbf{r})$, where $f(\mathbf{r})$ satisfies the Schrödinger equation. Since $u(\mathbf{r})$ is even for the valence band states but odd for the conduction band states, an interband one-photon transition is allowed when its initial and final state envelope functions have the same parity (i.e. s shell- s shell and p shell- p shell transitions, as shown in Fig. 2b)[26], while an interband two-photon transitions is allowed when its initial and final state envelope functions have the opposite parity (i.e. s shell- p shell transition and vice versa, as shown in Fig. 2c).

To solve this problem, we propose the application of lateral electric fields to break the parity symmetry in wavefunctions. Recent experiments have demonstrated the Stark shift of QD transitions in bulk[27], as well as in photonic crystal cavities[28, 29]. Following Refs. [30] and [27], we model the QD as a particle in a finite well along its growth axis and a two-dimensional harmonic oscillator perpendicular to its growth axis. We denote the electron (hole) effective mass and oscillator frequency as m_e^* and ω_e (m_h^* and ω_h). For the one-photon s shell- s shell transition, the lateral electric field \mathcal{E} reduces this transition dipole moment with expression $\mathbf{d}_{ge} = e\mathbf{r}_{cv} \exp[-(\Delta x)^2/(4l_e^2)]$, where $\mathbf{r}_{cv} = \int_V d\mathbf{r} u_c(\mathbf{r})\mathbf{r}u_v(\mathbf{r})$ is the transition moment between the valence band and the conduction band integrated over an unit cell, $\Delta x = e\mathcal{E}[(m_e^*\omega_e^2)^{-1} + (m_h^*\omega_h^2)^{-1}]$ is the separation of the electron and hole wavefunction centers, and $l_e = l_h = \sqrt{\hbar/(2m_e^*\omega_e)}$ is the oscillator length. For the two-photon s shell- s shell transition, the predominant intermediate states are the conduction and valence p shell states. Consider the case of $|k\rangle = \text{conduction } p \text{ shell}$, we have $|\mathbf{d}_{gk}| = e|\mathbf{r}_{cv}|(\Delta x/l_e) \exp[-(\Delta x)^2/(4l_e^2)]$, $|\mathbf{d}_{ke}| = el_e$, and therefore $|\mathbf{d}_{gk}||\mathbf{d}_{ke}| = e^2|\mathbf{r}_{cv}|\Delta x \exp[-(\Delta x)^2/(4l_e^2)]$. The case of $|k\rangle = \text{valence } p \text{ shell}$ gives the same product of transition dipole moments.

Fig. 3a shows the enhanced TPA effective Rabi rate $\Omega_{\text{eff}}/2\pi$ (Eqn. (1)), enhanced TPSE rate $\Gamma_{\omega_1, \omega_2}^{\text{TPSTE}}/2\pi$ (Eqn. (5)), and one-photon spontaneous emission rate $\gamma^{\text{OPSE}}/2\pi$ as a function of lateral electric field. The simulation parameters are

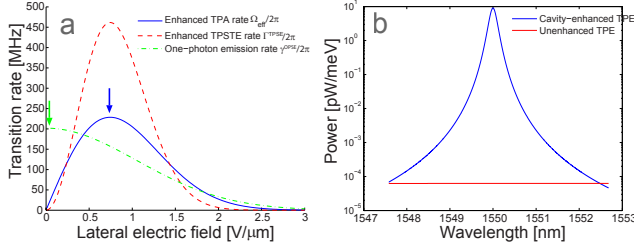


FIG. 3: (Color online) (a) Cavity-enhanced two-photon absorption effective Rabi rate (blue solid line), enhanced two-photon stimulated emission rate (red dashed line), and one-photon spontaneous emission rate (green dash-dot line) as a function of lateral electric field strength. All of the transitions are s shell- s shell. The simulation parameters are shown in text. (b) Cavity-enhanced two-photon spontaneous emission power (blue) and unenhanced emission power (red) of 1550 nm photons. Pairs of photons of 1550 nm and 2300 nm wavelength are emitted from the excited QD.

$m_h^* = 2m_e^* = 0.11m_0$ (m_0 is the electron rest mass), $\hbar\omega_e = 2\hbar\omega_h = 12$ meV[30], $|\mathbf{r}_{cv}| = 0.6$ nm[31], $\eta_1 = \eta_2 = 2\%$, $Q_1 = Q_2 = 5000$, $V_i = (\lambda_i/n)^3$, $\phi's = 1$, and $\psi's = 1$. $P_1 = P_2 = 12$ μ W for enhanced TPA and $P_2 = 100$ μ W for enhanced TPSTE. The assumed low incoupling efficiencies of 2% are taken from the experiments where the input laser beam is coupled to the cavity in the direction perpendicular to the chip[6, 7, 8]. However, it must be pointed out that PC cavities coupled to fiber tapers or PC waveguide can achieve a coupling efficiency of 70-90%[32, 33] and therefore lower the needed external excitation power. For enhanced TPA and subsequent single photon generation (Fig. 2d), we operate in the region where $\mathcal{E} < 0.5$ V/ μ m with $\Omega_{\text{eff}} < \gamma^{\text{OPSE}}$ to prevent Rabi oscillations between the ground and excited states. The electric field of 1 V/ μ m strength only shifts the s shell- s shell transition by approximately 0.1 nm[27], and therefore the QD is still on resonance with the double-mode cavity. In the case that the cavity also possesses a resonance mode at 926 nm, the single photon generation rate will be further enhanced by the Purcell factor at this mode. For enhanced TPSTE used to generate 1550 nm single photons, we operate in the region such that $\Gamma_{\omega_{1c}, \omega_{2c}}^{\text{TPSTE}} > \gamma^{\text{OPSE}}$ to prevent 926 nm one-photon spontaneous emission of the excited QD. This implies that $\mathcal{E} > 0.3$ V/ μ m.

In addition to the application of a static electric field, a modulation of electric field can change the parity selection rules dynamically. For example, we keep the electric field on at approximately 0.75 V/ μ m to enable the s shell- s shell excitation via TPA (Fig. 3a blue arrow), but then turn off the field to permit a rapid single photon emission (Fig. 3a green arrow). This way we can permit both an efficient excitation and an efficient photon emission, because this approach allows for maximum transition rates in both steps. For an estimation of the modulation speed, we need to switch the electric field on a timescale that is faster than the recombination rate for an excited QD, which is 100 ps-1 ns. Today's commercial function generators can easily achieve this speed.

Fig. 3b shows the power of 1550 nm photons emitted by enhanced two-photon spontaneous emission. The figure shows that the peak enhanced TPSE power from a single QD is on the same order as the power from a 200- μ m-thick GaAs sample with carrier concentration of 1.2×10^{18} cm $^{-3}$ [22].

In conclusion, we have derived the expressions for enhancement of two-photon spontaneous emission, two-photon stimulated emission, and two-photon absorption from a single QD in an optical nanocavity. Up to 8 orders of magnitude in rate enhancement is possible. We have also discussed how this could be applied to several important challenges in quantum information science. In particular, enhanced two-photon absorption allows coherent excitation of quantum dots and eliminates jitter, thus enabling generation of indistinguishable single photons on demand; enhanced two-photon spontaneous emission generates entangled photon pairs in polarization; enhanced two-photon stimulated emission further increases the emission rate and allows single photon generation at telecom wavelengths.

Although we use semiconductor QDs as an illustration for cavity enhanced TPA and TPE in this paper, we can use the same approach to excite and manipulate other emitters such as 637 nm nitrogen-vacancy centers by laser beams in the 1550 nm telecom range. The cavity enhanced TPA and TPE can even enable construction of hybrid quantum networks containing different emitters just by changing the frequency of one of the excitation lasers.

The authors gratefully acknowledge financial support provided by National Science Foundation and the Army Research Office. Z. L. was supported by the NSF Graduate Fellowship and Stanford Graduate Fellowship.

* Electronic address: carterlin@stanford.edu

- [1] D. Englund et al., Opt. Express **15**, 5550 (2007).
- [2] S. Laurent et al., Appl. Phys. Lett. **87**, 163107 (2005).
- [3] D. Englund et al., Phys. Rev. Lett. **95**, 013904 (2005).
- [4] K. Hennessy et al., Nature **445**, 896 (2007).
- [5] T. Yoshie et al., Phys. Rev. Lett. **432**, 200 (2004).
- [6] D. Englund et al., Nature **450**, 857 (2007).
- [7] I. Fushman et al., Science **320**, 769 (2008).
- [8] A. Faraon et al., Nat. Phys. **4**, 859 (2008).
- [9] J. I. Cirac et al., Phys. Rev. Lett. **78**, 3221 (1997).
- [10] L.-M. Duan et al., Nature **414**, 413 (2001).
- [11] L.-M. Duan et al., Phys. Rev. Lett. **92**, 127902 (2004).
- [12] J. Vuckovic et al., Physica E **2**, 466 (2006).
- [13] C. Becher et al., Physica E **13**, 412 (2002).
- [14] C. Santori et al., Nature **419**, 594 (2002).
- [15] O. Benson et al., Phys. Rev. Lett. **84**, 2513 (2000).
- [16] N. Akopian et al., Phys. Rev. Lett. **96**, 130501 (2006).
- [17] R. M. Stevenson et al., Nat. Phys. **439**, 179 (2005).
- [18] D. Gammon et al., Phys. Rev. Lett. **76**, 3005 (1996).
- [19] M. Bayer et al., Phys. Rev. B **65**, 195315 (2002).
- [20] L. A. Padilha et al., Phys. Rev. B **75**, 075325 (2007).
- [21] G. Xing et al., Appl. Phys. Lett. **93**, 241114 (2008).
- [22] A. Hayat et al., Nat. Photonics **2**, 238 (2008).
- [23] E. M. Purcell, Phys. Rev. **69**, 674 (1946).

- [24] J. Vuckovic et al., Phys. Rev. E **65**, 016608 (2001).
- [25] D. Englund et al. (2009), arXiv:0902.2428v2.
- [26] P. Michler, *Single Quantum Dots: Fundamentals, Applications and New Concepts* (Springer, 2003).
- [27] M. E. Reimer et al., Phys. Rev. B **78**, 195301 (2008).
- [28] A. Laucht et al., New J. Phys. **11**, 023034 (2009).
- [29] A. Faraon et al. (2009), arXiv:0906.0751.
- [30] M. Korkusinski et al., Phys. Rev. B **79**, 035309 (2009).
- [31] P. G. Eliseev et al., Appl. Phys. Lett. **77**, 262 (2000).
- [32] I.-K. Hwang et al., Appl. Phys. Lett. **87**, 131107 (2005).
- [33] A. Faraon et al., Appl. Phys. Lett. **90**, 073102 (2007).